AGU PUBLICATIONS

Geophysical Research Letters

RESEARCH LETTER
10.1002/2015GL065782

Key Points:
- Modeled restructuring of the Siple Coast ice streams replicates past flow features
- Kamb Ice Stream tributaries are the source of regional ice flow instability
- Reduced regional mass balance could increase sea level by 5 mm in 100 years

Supporting Information:
- Texts S1–S3, Figures S1–S3, and Tables S1–S3

Correspondence to:
M. Bougamont,
mb627@cam.ac.uk

Citation:
Bougamont, M., P. Christoffersen, S. F. Price, H. A. Fricker, S. Tulaczyk, and S. P. Carter (2015), Reactivation of Kamb Ice Stream tributaries triggers century-scale reorganization of Siple Coast ice flow in West Antarctica, *Geophys. Res. Lett.*, *42*, 8471–8480, doi:10.1002/2015GL065782.

Received 12 AUG 2015
Accepted 25 SEP 2015
Accepted article online 29 SEP 2015
Published online 21 OCT 2015

Reactivation of Kamb Ice Stream tributaries triggers century-scale reorganization of Siple Coast ice flow in West Antarctica

M. Bougamont[1], P. Christoffersen[1], S. F. Price[2], H. A. Fricker[3], S. Tulaczyk[4], and S. P. Carter[3]

[1]Scott Polar Research Institute, University of Cambridge, Cambridge, UK, [2]Fluid Dynamics and Solid Mechanics Group, Los Alamos National Laboratory, Los Alamos, New Mexico, USA, [3]Scripps Institute of Oceanography, University of California, San Diego, La Jolla, California, USA, [4]Department of Earth and Planetary Sciences, University of California, Santa Cruz, California, USA

Abstract Ongoing, centennial-scale flow variability within the Ross ice streams of West Antarctica suggests that the present-day positive mass balance in this region may reverse in the future. Here we use a three-dimensional ice sheet model to simulate ice flow in this region over 250 years. The flow responds to changing basal properties, as a subglacial till layer interacts with water transported in an active subglacial hydrological system. We show that a persistent weak bed beneath the tributaries of the dormant Kamb Ice Stream is a source of internal ice flow instability, which reorganizes all ice streams in this region, leading to a reduced (positive) mass balance within decades and a net loss of ice within two centuries. This hitherto unaccounted for flow variability could raise sea level by 5 mm this century. Better constraints on future sea level change from this region will require improved estimates of geothermal heat flux and subglacial water transport.

1. Introduction

Antarctic ice streams transfer ice from the continental interior to the ocean, and their flow dictates the mass balance of the ice sheet. Between 1992 and 2011, the Antarctic ice sheet lost $71 \pm 53\,\mathrm{Gt\,yr^{-1}}$ [*Jenkins et al.,* 2010; *Shepherd et al.,* 2012] as a result of ice streams in the Amundsen region accelerating in response to oceanic warming [*Jenkins et al.,* 2010; *Paolo et al.,* 2015]. About 43% of the net loss of ice from this sector ($-83 \pm 5\,\mathrm{Gt\,yr^{-1}}$ in 1992–2013) [*Sutterley et al.,* 2014] is countered by ice flow within the Siple Coast (Figure 1a), where the regional mass balance is currently positive ($36 \pm 16\,\mathrm{Gt\,yr^{-1}}$ in 2003–2007) [*Pritchard et al.,* 2009]. This follows the stagnation of Kamb Ice Stream (KIS) about 170 years ago, combined with the ongoing slowdown of Whillans Ice Stream (WIS) [*Joughin and Tulaczyk*, 2002; *Beem et al.*, 2014], which could increase the positive mass balance to $+57\,\mathrm{Gt\,yr^{-1}}$ if slowdown continues to stagnation [*Joughin and Tulaczyk*, 2002]. Subtler changes are taking place on the neighboring Bindschadler (BIS) and MacAyeal (MacIS) ice streams, which accelerated and decelerated by $+20\,\mathrm{m\,yr^{-1}}$ and $-30\,\mathrm{m\,yr^{-1}}$ respectively, between 1997 and 2009 [*Scheuchl et al.,* 2012]. Reconstruction of past ice flow, based on streak lines on the Ross Ice Shelf [*Hulbe and Fahnestock*, 2007] and relict features on and near ice streams [*Catania et al.,* 2012], shows century-scale fluctuations of all ice streams in this region, including Siple Ice Stream (SIS), which stopped 450 years ago [*Jacobel et al.,* 2000] and has remained stagnant since [*Catania et al.,* 2012].

Variability in ice flow along the Siple Coast is largely controlled by internal processes whereby subglacial hydrology, basal processes and thermal regimes, and migration of lateral shear margins all contribute to the overall speed and location of streaming ice [*Raymond*, 2000; *Schoof*, 2004; *Joughin and Alley*, 2011; *Beem et al.*, 2014]. The interplay between these processes is complex and poorly understood, making estimate of future ice flow changes in this region challenging and highly uncertain. Consequently, this potential future variability is typically ignored in sea level projections [*Church et al.,* 2013], which assume that ice discharge from the Siple Coast ice streams will continue to counteract sea level rise (SLR) at the same rate during the 21st century and beyond.

Here we use the three-dimensional Community Ice Sheet Model (CISM) coupled to dynamic subglacial hydrology and basal processes submodels to simulate the evolution of all five Siple Coast ice streams over a 250 year period. When ice flow and basal hydromechanical processes are coupled, the model demonstrates

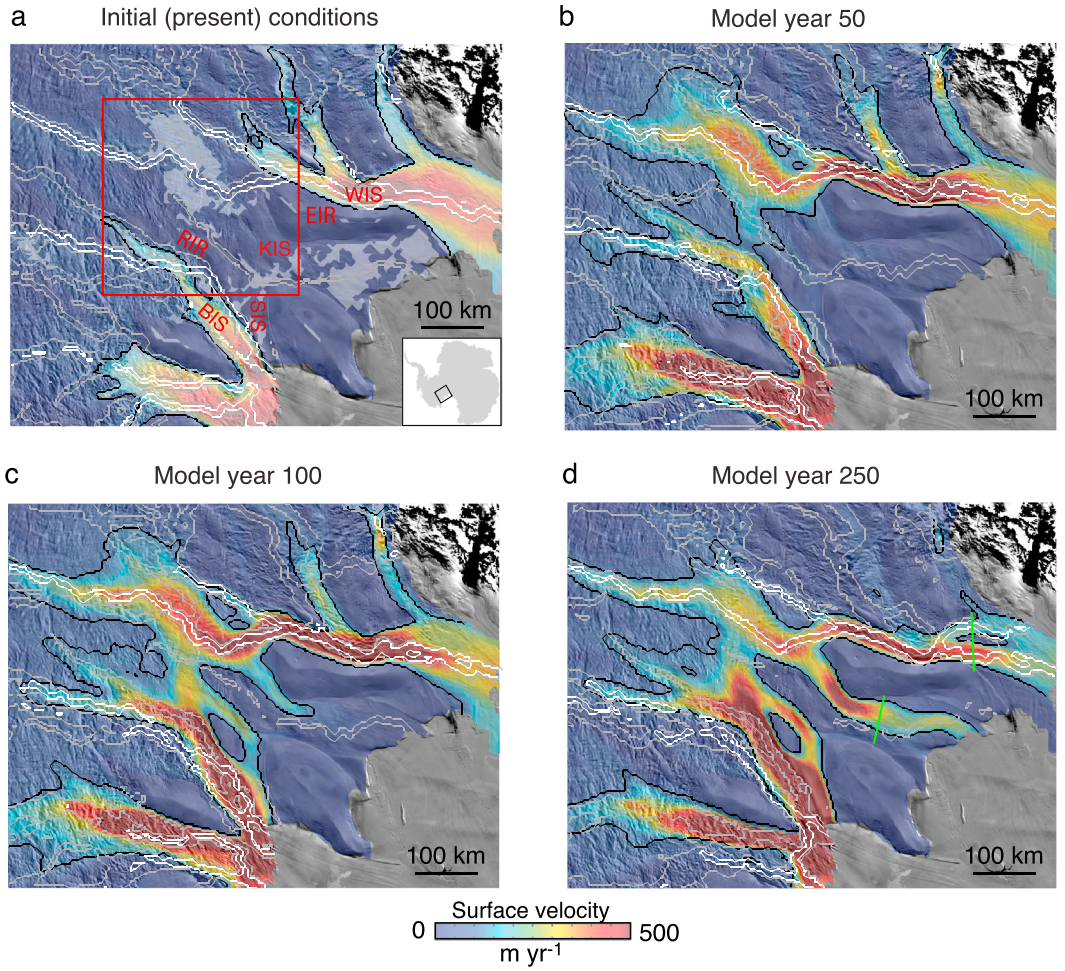

Figure 1. Location of Whillans Ice Stream (WIS), Kamb Ice Stream (KIS), Bindschadler Ice Stream (BIS), Engelhardt Ice Ridge (EIR), and Raymond Ice Ridge (RIR), shown on maps of modeled surface velocity (m yr^{-1}), overlain with the 100 m yr^{-1} velocity contour (black), and hydrological fluxes contours (1 m^3 yr^{-1} in gray and 5 m^3 yr^{-1} in white). Output of the Inland_Flux experiment shown for (a) initial conditions, (b) model year 50, (c) model year 100, and (d) model year 250. In addition, the white shaded area in Figure 1a indicates where the initial driving stress exceeds the initial modeled basal drag. This covers all the fast flow regions, plus large sections of KIS. Subset used in Figure 2 is identified in red in Figure 1a, and profiles used in Figure 3 are shown in green in Figure 1d.

"piracy" of ice and water between neighboring ice streams, which results in ice stream stagnation and reactivation, consistent with reconstructions of their past flow based on observations [*Price et al.*, 2001; *Conway et al.*, 2002; *Catania et al.*, 2012]. We show that a regional ice flow instability, which influences all the major ice streams on the Siple Coast, is centered in the tributaries of KIS, where basal resistance is inferred to be weak [*Kamb*, 2001; *Anandakrishnan*, 2003; *Catania et al.*, 2003; *Jacobel et al.*, 2009]. We analyze the hydromechanical and thermal processes involved in the restructuring of flow, and we discuss implications for the regional mass balance over the next two centuries.

2. Methods

2.1. Ice Flow Model

We use CISM [*Bougamont et al.,* 2011; *Price et al.,* 2011, 2015], a three-dimensional ice sheet model that predicts (i) ice thickness evolution by solving the mass conservation equation, (ii) temperature evolution by solving the advective-diffusive heat equation, and (iii) ice velocities by solving the conservation of momentum based on the first-order approximation to the Stokes equations for ice flow [*Blatter*, 1995; *Pattyn*, 2003; *Dukowicz et al.*, 2010]. The ice flow model is coupled to a basal processes model by determining

the porosity-controlled basal yield strength (Text S1 in the supporting information), using a plastic yield-stress basal boundary condition as in *Bueler and Brown* [2009]. A complete description of the ice sheet and basal processes models can be found in *Bougamont et al.* [2011].

2.2. Subglacial Hydrology and Till Layer

The modeled regional basal water system consists of water produced locally from basal melting plus water originating farther inland, and it coexists with a water-saturated basal till layer. Due to the efficiency of the hydrological system [*Kamb*, 2001] and low hydraulic diffusivity and conductivity of subglacial till [*Engelhardt and Kamb*, 1997], we treat each system in isolation and assume that water in the hydrological system is transported over long distances (e.g., across the model domain) before interacting with the subglacial till layer. First, we specify the hydrological path and flux with a model that successfully simulated the exchange of water between subglacial lakes at the base of the Siple Coast ice streams [*Carter and Fricker*, 2012], where water is routed according to gradients in hydraulic potential [*Shreve*, 1972]. As such, the pathway and flux of basal water evolve together with the ice geometry and the spatially distributed basal melt rate. We then calculate the distributed water film depth adjusted per time unit from the evolving water fluxes [*Le Brocq et al.,* 2009]. This water thickness is allowed into the subglacial till layer, which increases its porosity. Where applicable, the till porosity is reduced to satisfy freezing, with rates calculated from the basal energy balance. Finally, subglacial till properties are calculated using an empirical formulation that uniquely relates the till strength to its porosity [*Tulaczyk et al.*, 2000; *Christoffersen and Tulaczyk*, 2003; *Bougamont et al.*, 2011; *Robel et al.*, 2013]. More details on the regional hydrological model and its coupling to the subglacial processes model are given in Text S1.

2.3. Initial and Boundary Conditions

We obtained realistic initial flow conditions by assimilating the 1997 observed velocities [*Joughin et al.,* 1999] with the iterative inversion technique described in *Price et al.* [2011] and with outcome detailed in *Christoffersen et al.* [2014] (see also Text S2). This showed good agreement with observations for the surface velocity (3.2% averaged misfit), basal stress (within the range of observations) and temperature distribution (6% averaged misfit, Table S1 and Figure S1), excluding the KIS trunk region where thermal conditions have not yet adjusted to its relatively recent stagnation. Inferred basal conditions remain indeed suggestive of this ice stream's past fast flow, when effective advection of cold ice promoted freezing conditions at the bed [*Engelhardt*, 2004; *Joughin et al.,* 2004]. To address this in the model, we imposed a uniform velocity of $500\,\mathrm{m\,yr^{-1}}$ at the trunk of KIS during the model spin-up, which induced basal freezing conditions in the model, and showed good agreement with the ice temperature profile measured at the UpC site on KIS (Figure S1 and Text S2).

We ran the model with 5 km spatial resolution, keeping the surface accumulation [*Arthern et al.,* 2006], temperature [*Comiso*, 2000], and basal geothermal heat flux fields steady in time. Inland-sourced water entering the regional hydrology system was prescribed with a constant water flux at the domain boundaries (see section 2.4).

Because our study focuses on internal ice sheet instabilities, we maintained fixed grounding line positions in all of our model runs. This allowed us to isolate the impact of a physically based representation of the evolution of ice stream basal properties, which is a new aspect of ice sheet models used for sea level rise predictions. We note that grounding line positions along the Siple Coast appear to have remained relatively stable over time scale of decades [*Horgan and Anandakrishnan*, 2006], despite large variations in ice flow.

2.4. Experimental Setup

In our principal experiment ("Inland_Flux"), we prescribed the inland-sourced water at the domain boundaries according to the hydrological budget calculated for each Siple Coast ice streams and totaling $860 \times 10^6\,\mathrm{m^3\,yr^{-1}}$ [*Christoffersen et al.,* 2014]. The geothermal heat flux (GHF) was based on estimates from a global seismic model [*Shapiro and Ritzwoller*, 2004].

With four additional experiments (summarized in Table S2), we tested the model sensitivity to

1. doubling the prescribed inland water flux ("Inland_Flux_$\times 2$" experiment), thereby increasing water availability for subglacial till weakening and ice flow lubrication;
2. turning off the inflow of water from the interior ("Inland_Flux_$\times 0$" experiment) so that only locally produced basal meltwater was routed through the regional hydrological system;

3. turning off the routing of basal meltwater, so that basal properties evolved solely from local variations in the rate of basal melting or freezing ("Till-only" experiment), as assumed in earlier work [e.g., *Bougamont et al.*, 2003b]; and
4. substituting the seismic-based GHF distribution in Inland_Flux with a GHF distribution estimated from magnetic satellite data [*Maule et al.,* 2005] ("GHF-Maule" experiment).

3. Siple Coast Ice Flow Reorganization

In the Inland_Flux experiment, the modeled ice streams evolve over the 250 year period, according to feedbacks between water fluxes in the regional hydrological system, till properties, ice geometry, and the ice temperature distribution. The first departure from initial conditions (Figure 1a) occurs after a few decades, when ice flow in the KIS tributaries accelerates (model year 50; Figure 1b). Subsequently, ice starts flowing into the northern tributary of WIS, an "ice piracy" which sustains the fast flow of upstream WIS, whereas the main trunk slows down. Ice piracy also occurs to the north of the KIS tributaries, as the acceleration of flow transfers ice to BIS over Raymond Ice Ridge (RIR), where modeled basal resistance is weak (see section 4). Consequently, BIS experiences a southward shift of its margins and enhanced flow in its tributaries.

By model year 100 (Figure 1c), the trunk of KIS reactivates, but the cold basal conditions that developed after its stagnation slow this process down. Hence, the upper KIS region continues to transfer ice to WIS and increasingly over RIR, ultimately resulting in the reactivation of SIS. The merging of SIS with BIS near the grounding zone significantly increases the flux of ice across the grounding line in this region (Figure 4). Meanwhile, MacIS slows down and narrows from a southward shift of its northern margin.

At model year 250 (Figure 1d), SIS has reached velocities up to 430 m yr^{-1}, and the reactivation of KIS propagates throughout its main trunk. This coincides with slopes flattening above Engelhardt Ice Ridge (EIR), which reduces the transfer of ice into WIS, resulting in slower flow and a large southward jump of the northern WIS margin (decrease in ice stream width). BIS remains active with an increased flow speed throughout the 250 year run.

The model results presented above are supported by a number of features that are in line with observations: (1) ice piracy from KIS to WIS, consistent with ongoing flow changes in this region [*Price et al.*, 2001; *Conway et al.*, 2002], (2) continued and progressive slowdown of the main trunk of WIS from the onset of the experiment, as detected in recent velocity trends [*Joughin and Tulaczyk*, 2002; *Joughin et al.*, 2005; *Beem et al.*, 2014], (3) reactivation of SIS and KIS with shear margins corresponding well with the relict margins identified from radio-echo sounding measurements [*Jacobel et al.,* 1996], and (4) sustained fast flow of BIS, which is the only ice stream in this region for which there is no evidence of stagnation over the past 1000 years [*Catania et al.,* 2012]. In addition, the model produces a large margin jump for WIS in response to significant reduction in ice flux, similar to events preceding KIS shutdown [*Retzlaff and Bentley*, 1993; *Catania et al.*, 2006]. Significant variability in grounding line position could contribute further to marginal jumps [*Fried et al.,* 2014], although this is not included in our model.

The dynamic sequence of ice flow reorganization is a robust model feature in all sensitivity runs (Figure S2), and includes (1) acceleration of KIS tributaries and subsequent transfer of ice into WIS and BIS during the first 100 years (ice piracy), (2) a slower but prolonged activity of WIS due to supply of basal water as well as ice piracy from KIS, (3) narrowing and slowdown of MacIS, and (4) reactivation of SIS and KIS in the second half of the experiment.

4. Partitioning Mechanical, Hydrological, and Thermal Drivers of Ice Flow Instability

In all experiments, we attribute the source of regional ice flow variability to the persistently weak basal conditions beneath the tributaries of KIS (Figure 1a). To understand the cause of this instability, we examine how ice flow is linked to mechanical, hydrological, and thermal properties at the bed. In particular, we use $\Delta\tau$, defined as the gravitational driving stress (e.g., the product of ice density, ice thickness, and acceleration due to gravity) minus basal drag (defined as the sum of all resistive stresses at the ice base), as a criterion to identify basal conditions for fast ice streaming, as the latter can only develop where $\Delta\tau > 0$, when significant resistance to flow comes from shear margins and longitudinal stress gradients. Based on the observed

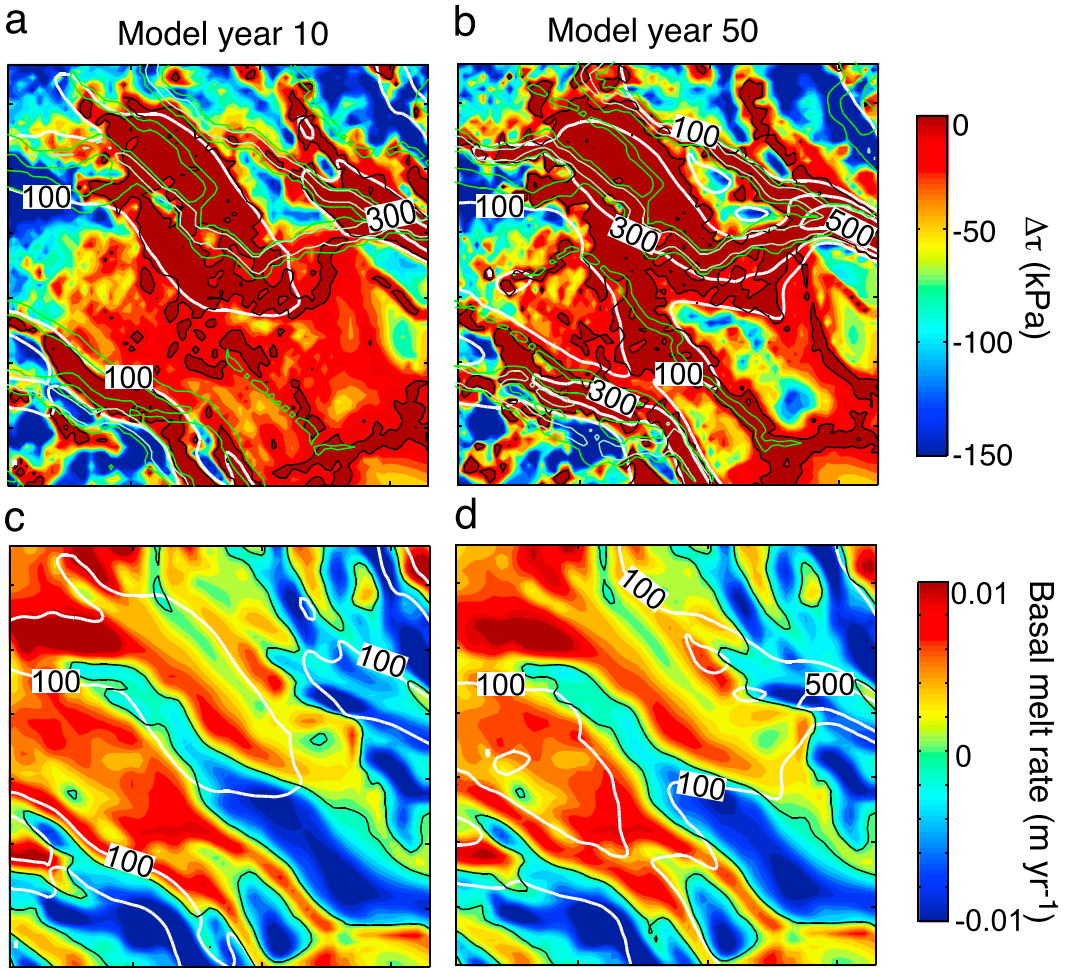

Figure 2. Results for the Inland_Flux experiment, showing the evolving surface velocity (white contours and labels, m yr^{-1}), with (a and b) the distributed values of driving stress minus basal drag ($\Delta\tau$, with 0 value contour in black). Also shown is the water flux in the regional hydrological system (1 m^3 yr^{-1} in dark green, and 5 m^3 yr^{-1} in light green) and (c and d) distribution of basal melt rate, with the 0 value contour in black.

1997 surface motion, the initialized model features a weak bed beneath the tributaries (Figure 1a) with $\Delta\tau \sim 15$ kPa, which is in good agreement with borehole measurements at the UpC site, located at the junction of the tributaries and trunk (measured $\Delta\tau \sim 5$–15 kPa) [*Kamb*, 2001]. This means that the current slow but enhanced flow of KIS tributaries (40 to 70 m yr^{-1}) occurs in a region where the basal conditions favor higher (>100 m yr^{-1}) velocities. Consequently, modeled ice flow in this region accelerates. More specifically, we find a close match between the 100 m yr^{-1} surface velocity contour and the contour defined as $\Delta\tau = 0$ (Figures 2a and 2b), regardless of the thermal regime (Figures 2c and 2d). Weak basal conditions are also identified as patches of positive $\Delta\tau$ near ridges EIR and RIR (Figure 2a), explaining why fast flow subsequently develops there (Figure 2b) rather than in the main trunk of KIS as anticipated [*Vogel et al.,* 2005].

To further assess how rapid, centennial-scale changes occur in the model, we analyzed the interconnected flow regime of KIS and WIS by examining the simultaneous evolution of ice velocity, basal energy budget, hydrological fluxes, and $\Delta\tau$ (Figure 3) for two 100 km long, across-flow transects (see Figure 1d for location). Persistent basal freezing beneath WIS (Figure 3c) causes slowdown due to dewatering and strengthening of the basal till layer, a widely discussed thermal effect acting over time scales of hundreds to thousands of years [*Christoffersen and Tulaczyk*, 2003; *Bueler and Brown*, 2009; *Bougamont et al.*, 2011; *Robel et al.*, 2013]. Superimposed on this effect are a rapid increase in driving stress (and therefore also $\Delta\tau$) as well as efficient lubrication supplied from the regional hydrology system, all of which modulate the flow on shorter time

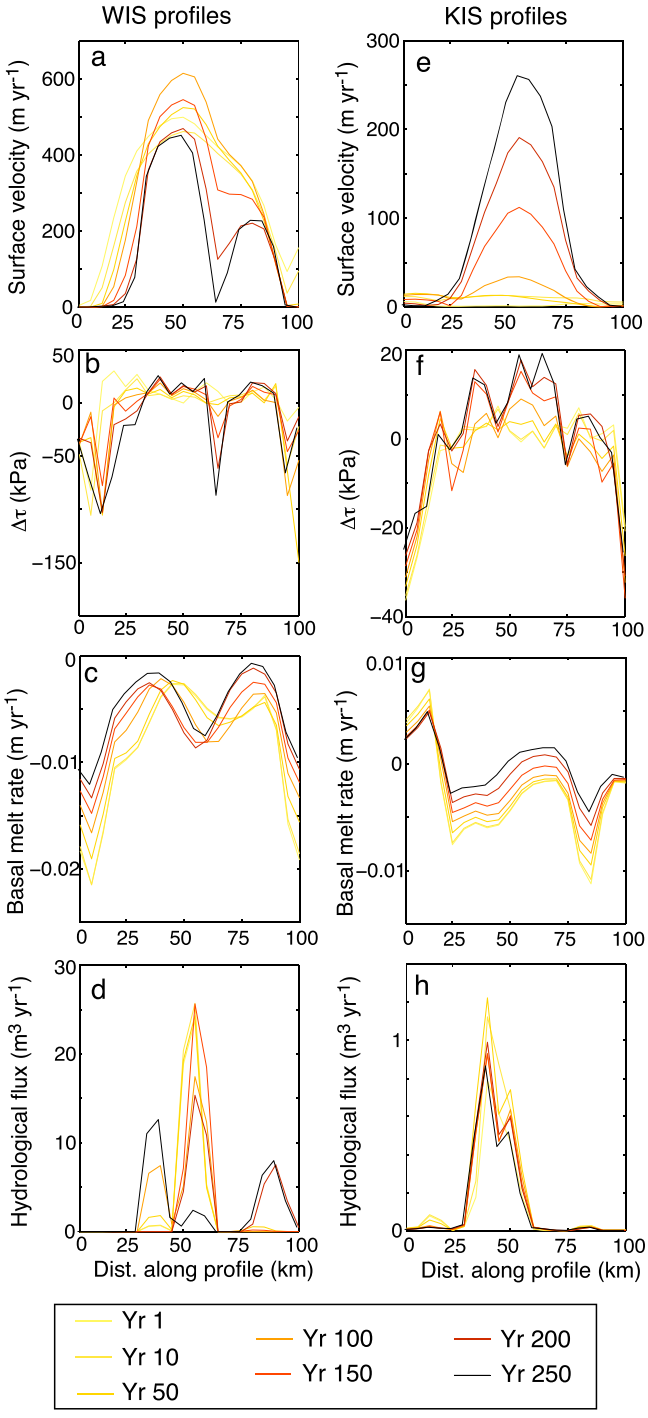

Figure 3. Results for the Inland_Flux experiment, showing (a and e) surface velocity, (b and f) driving stress minus the basal drag, (c and g) basal melt rate, and (d and h) regional hydrological flux, along transects located on WIS (Figures 3a–3d) and KIS (Figures 3e–3h), for model years as shown in the legend. Transect locations are indicated in Figure 1d. Ice flow is in the out-of-the-page direction.

scales (tens to hundreds of years). For example, the central section of WIS (km 35 to km 60 of the profile) undergoes 100 years of flow acceleration (Figure 3a), despite basal freezing (Figure 3c). This is due to increased driving stresses farther upstream as ice flows in from the KIS tributaries (as seen in Figure 1) and also due to basal water fluxes of ~10–25 $m^3 yr^{-1}$ in the regional hydrology system (Figure 3d), which buffer basal freezing. Ice flow acceleration on the WIS stops when the main trunk of KIS reactivates (from model year 100; Figures 1c and 3e), because ice flow then reverts from the upper WIS back into the KIS catchment, reducing the supply of ice to the trunk of WIS. Efficient routing of water in the hydrological system also plays a key role in defining the new position of the WIS northern margin, which migrates south to reach km 25 along the profile (Figure 3a), where the surface velocity drops from 350 $m yr^{-1}$ to $<10 m yr^{-1}$. Indeed, freezing in a subglacial setting without external water inputs between km 0 and km 25 results in till consolidation and bed strengthening ($\Delta\tau < 0$; Figure 3b). However, continuously active hydrology at km 30 (Figure 3d) prevents basal strengthening and marks the new marginal limit of active flow. Finally, basal conditions defined by lack of external water inputs lead to localized high basal friction at km 65 ($\Delta\tau < 0$; Figure 3b), producing a "sticky spot" over which velocity drops from 400 $m yr^{-1}$ to values consistent with no enhanced basal flow ($<10 m yr^{-1}$). This sticky spot, consisting of an island of stagnant ice surrounded by fast flow, is similar to that currently observed on KIS [*Anandakrishnan and Alley,* 1994, 1997; *Jacobel et al.,* 2009].

Likewise, the flow of the main trunk of KIS experiences rapid (tens to hundreds of years) variations, which cannot be explained solely by changes in the basal heat budget. The main trunk reactivates (Figure 3e) under basal freezing conditions (Figure 3g), which demonstrates that a reversal to basal melting is not a prerequisite for reactivation. In our model, the reactivation occurs following an increase in $\Delta\tau$ from ~0 to >10 kPa (Figure 3f), which is largely attributed to higher

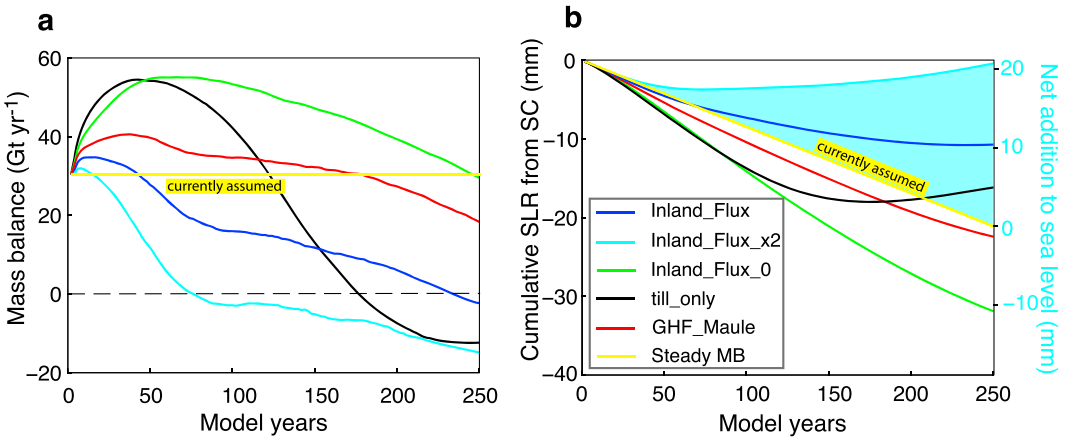

Figure 4. (a) Modeled mass balance of the Siple Coast (SC) region and (b) associated cumulative sea level rise relative to present (left-hand side axis). Results are shown for Inland_Flux (dark blue), Inland_Flux_ × 2 (cyan), Inland_Flux_ × 0 (green), Till-only (black), and GHF-Maule (red) experiments. Projections assuming no changes in mass balance from present conditions are labeled Steady MB (yellow). Lowering the mass balance reduces the counterbalance to SLR currently provided by the SC region, and the associated net effect is an increased sea level (right-hand side axis, shaded blue area).

driving stress resulting from a buildup of ice at the confluence of the active tributaries and the stagnant trunk. This feedback between ice flow dynamics and geometry is seen in all sensitivity experiments and is in line with observations in that sector [*Price et al.,* 2001]. We further note that reactivation of the main trunk of KIS increases frictional heating, which *then* helps restore basal melting conditions (rather than the opposite) (Figures 3e and 3g). The modeled reactivation of the main trunk of KIS occurs with active margins positioned where $\Delta\tau < 0$ (Figure 3f). Outside the northern margin, basal melting is constant throughout the run, but the process is too slow to allow a switch in flow regime on centennial time scale.

5. Variability of the Siple Coast Mass Balance Over the Next 250 Years

For all model runs, we estimated the long-term regional mass balance from the ice flux passing through gates as defined in *Joughin and Tulaczyk* [2002] (see also Figure S1). Although the main sequence of events was similar in all runs (section 3 and Figure S2), small differences became significant when considering the integrated impact on the regional mass balance (Figure 4 and Text S3).

If there were no changes in ice discharge from present conditions, the Siple Coast region would reduce global sea level by ~20 mm over the next 250 years (based on a discharge of ~30 Gt yr^{-1} estimated in *Joughin and Tulaczyk* [2002]). By cumulating rates of mass balance calculated throughout the simulations, our results indicate an actual reduction in global sea level ranging from 32 mm (Inland_Flux_ × 0) to just 0.5 mm (Inland_Flux_ × 2). In the baseline experiment Inland_Flux, we find that the mass balance drops below current estimates by model year 50 and becomes negative before the end of the experiment. In the Till-only experiment, the large amplitude of mass balance variation stems from (1) a reduced outflow earlier in the experiment, as basal freezing increases the bed resistance of all ice stream trunks (Figure S1) and (2) an increased discharge when SIS merges with BIS (Figure S2). In contrast, active hydrology in the Inland_Flux, Inland_Flux_ × 2, and GHF-Maule experiments provides a buffer to freezing, which limits the reduction in ice discharge early in the experiment. Finally, uncertainties in GHF have a large impact in transient ice flow experiments, here resulting in a factor 2 difference in cumulative SLR over 250 years.

6. Conclusions

Using a higher-order ice flow model with a dynamic parameterization of the basal interface, we produced the first realistic simulation of complex and unstable ice flow in the Siple Coast region of West Antarctica. While recent work has focused on these ice streams shutting down further in the near future [*Bougamont et al.,* 2003a; *Joughin et al.,* 2005], our results suggest that the associated positive state of mass balance is only temporary because a source of regional ice sheet instability is located in the upper region of KIS where basal resistance is inferred to be weak [*Anandakrishnan*, 2003; *Catania et al.,* 2003; *Jacobel et al.,* 2009]. In the model,

the consequence of this instability is a major flow restructuring for all of the Siple Coast ice streams over a period of tens to hundreds of years. The robustness of the model results is demonstrated by the dynamic, yet persistent flow patterns, obtained in a series of experiments with varying basal boundary conditions, and by detailed model features that accurately capture present and past flow characteristics [*Price et al.*, 2001; *Conway et al.*, 2002; *Catania et al.*, 2012]. The connectivity between each ice stream drainage system is a key element of the flow reorganization, as is the transfer of ice from distant locations and the associated geometrical changes. In our simulations, changes in mass flux on time scales of decades are sufficient to trigger catchment-scale flow variability, with downstream propagation that follows the path of "weakest basal resistance". As such, hydrological pathways determined new marginal positions in several instances. The mass balance results underscore how regional hydrology exerts a major control on the regional mass balance, not only by damping the thermally imposed oscillatory behavior of ice streams [*van der Wel et al.,* 2013] but also by promoting fast flow and maintaining an overall higher ice discharge over time. In current projections, the mass balance of the Siple Coast is often assumed to be invariant during the 21st century [*Church et al.,* 2013]. Our results show that accounting for the century-scale ice flow variability tied to internal processes in this region could reduce the mass balance from +30 Gt yr^{-1} today down to −3 Gt yr^{-1} by year +100, effectively adding up to ~5 mm of sea level rise during the next century. Averaged over this period, this translates in an annual contribution of 0.05 mm yr^{-1} or 25% of the current rate of SLR from the entire Antarctic ice sheet (0.20 mm yr^{-1}) [*Shepherd et al.,* 2012].

The ice flow model includes a higher-order momentum balance, which embeds the physics considered to be central for capturing the spatial shift from shearing in the horizontal plane to shearing in the vertical [*Whillans and van der Veen*, 2001; *Pattyn*, 2003; *Van der Veen et al.*, 2007] and for accommodating a nonlocal flow response to basal and/or geometrical changes [*Raymond et al.*, 2001; *Price et al.*, 2002]. No additional physics were needed to account for marginal conditions in a transition zone where the ice velocity drops by 2–3 orders of magnitude over a distance of only a few kilometers (e.g., less than the model resolution), and shear margin migration in the model corresponds well with characteristic flow signatures, such as those observed for SIS. Although we cannot exclude the possibility that processes not included in our model may be important [*Jacobson and Raymond*, 1998; *Raymond et al.*, 2001; *Schoof*, 2004; *Suckale et al.*, 2014], the use of higher-order physics appears to accommodate the well-known mobility of shear margins in this work.

A number of elements are still poorly constrained in our understanding of the subglacial environment, including the volume of water produced and transferred across the domain and its level of hydrological coupling with the till layer. While the sensitivity experiments performed here clearly show that active subglacial hydrology leads to greater ice discharge over time, the range of calculated contribution to SLR remains large and underscores the need to maintain efforts to characterize the basal environment of ice streams from observations [*Christianson et al.,* 2012; *Christoffersen et al.,* 2014; *Siegfried et al.,* 2014; *Tulaczyk et al.,* 2014] and their representation in numerical models. For instance, future model development could aim at accounting for subglacial lake activity [*Carter and Fricker*, 2012], for more accurate coupling between the water flow and the ice [*Kyrke-Smith et al.,* 2014], or processes leading to the channelization of water flow [*van der Wel et al.,* 2013]. Such developments would also help understanding how the overall ice flow is affected by local instabilities in basal drag linked to the presence of water [*Sergienko and Hindmarsh*, 2013; *Arthern et al.,* 2015]. Finally, the sensitivity to GHF values in transient ice flow experiments strongly suggests that a better quantification of this highly uncertain subglacial property may be crucial for accurate prediction of future sea level rise from the West Antarctic Ice Sheet.

Acknowledgments

This work was carried out with support from the Isaac Newton trust, Cecil H., and Ida M. Green Foundation and Natural Environment Research Council (grants NE/E005950/1 and NE/J005800/1). S.F.P. was supported by the U.S. Department of Energy Office of Science, Biological and Environmental Research program. S.T. acknowledges support from National Science Foundation (grant #0338295). S.P.C. was supported by funding from the Cryospheric Sciences program of NASA, and H.A.F. was supported by funding from NSF (grant ANT-0838885 (Fricker)). The source code for the results presented can be obtained by contacting the corresponding author directly.

References

Anandakrishnan, S. (2003), Dilatant till layer near the onset of streaming flow of Ice Stream C, West Antarctica, determined by AVO (amplitude vs offset) analysis, *Ann. Glaciol.*, *36*, 283–286.

Anandakrishnan, S., and R. B. Alley (1994), Ice Stream-C, Antarctica, sticky spots detected by microearthquake monitoring, in *Proceedings of the Fifth International Symposium on Antarctic Glaciology*, *Ann. Glaciol.*, vol. 20, edited by E. M. Morris, pp. 183–186, Int. Glaciol. Soc., Cambridge, U. K.

Anandakrishnan, S., and R. B. Alley (1997), Stagnation of ice stream C, West Antarctica by water piracy, *Geophys. Res. Lett.*, *24*(3), 265–268, doi:10.1029/96GL04016.

Arthern, R. J., D. P. Winebrenner, and D. G. Vaughan (2006), Antarctic snow accumulation mapped using polarization of 4.3-cm wavelength microwave emission, *J. Geophys. Res.*, *111*, D06107, doi:10.1029/2004JD005667.

Arthern, R. J., R. C. A. Hindmarsh, and C. R. Williams (2015), Flow speed within the Antarctic ice sheet and its controls inferred from satellite observations, *J. Geophys. Res. Earth Surf.*, *120*, 1171–1188, doi:10.1002/2014JF003239.
Beem, L. H., S. M. Tulaczyk, M. A. King, M. Bougamont, H. A. Fricker, and P. Christoffersen (2014), Variable deceleration of Whillans Ice Stream, West Antarctica, *J. Geophys. Res. Earth Surf.*, *119*, 212–224, doi:10.1002/2013JF002958.
Blatter, H. (1995), Velocity and stress-fields in grounded glaciers: A simple algorithm for including deviatoric stress gradients, *J. Glaciol.*, *41*(138), 333–344.
Bougamont, M., S. Tulaczyk, and I. Joughin (2003a), Numerical investigations of the slow-down of Whillans Ice Stream, West Antarctica: Is it shutting down like Ice Stream C?, *Ann. Glaciol.*, *37*, 239–246.
Bougamont, M., S. Tulaczyk, and I. Joughin (2003b), Response of subglacial sediments to basal freeze-on 2. Application in numerical modeling of the recent stoppage of Ice Stream C, West Antarctica, *J. Geophys. Res.*, *108*(B4), 2223, doi:10.1029/2002JB001936.
Bougamont, M., S. Price, P. Christoffersen, and A. J. Payne (2011), Dynamic patterns of ice stream flow in a 3-D higher-order ice sheet model with plastic bed and simplified hydrology, *J. Geophys. Res.*, *116*, F04018, doi:10.1029/2011JF002025.
Bueler, E., and J. Brown (2009), Shallow shelf approximation as a "sliding law" in a thermomechanically coupled ice sheet model, *J. Geophys. Res.*, *114*, F03008, doi:10.1029/2008JF001179.
Carter, S. P., and H. A. Fricker (2012), The supply of subglacial meltwater to the grounding line of the Siple Coast, West Antarctica, *Ann. Glaciol.*, *53*(60), 267–280, doi:10.3189/2012AoG60A119.
Catania, G., C. Hulbe, H. Conway, T. A. Scambos, and C. F. Raymond (2012), Variability in the mass flux of the Ross ice streams, West Antarctica, over the last millennium, *J. Glaciol.*, *58*(210), 741–752, doi:10.3189/2012JoG11J219.
Catania, G. A., H. B. Conway, A. M. Gades, C. F. Raymond, and H. Engelhardt (2003), Bed reflectivity beneath inactive ice streams in West Antarctica, *Ann. Glaciol.*, *36*, 287–291.
Catania, G. A., T. A. Scambos, H. Conway, and C. F. Raymond (2006), Sequential stagnation of Kamb Ice Stream, West Antarctica, *Geophys. Res. Lett.*, *33*, L14502, doi:10.1029/2006GL026430.
Christianson, K., R. W. Jacobel, H. J. Horgan, S. Anandakrishnan, and R. B. Alley (2012), Subglacial Lake Whillans—Ice-penetrating radar and GPS observations of a shallow active reservoir beneath a West Antarctic ice stream, *Earth Planet. Sci. Lett.*, *331*, 237–245, doi:10.1016/j.epsl.2012.03.013.
Christoffersen, P., and S. Tulaczyk (2003), Response of subglacial sediments to basal freeze-on 1. Theory and comparison to observations from beneath the West Antarctic Ice Sheet, *J. Geophys. Res.*, *108*(B4), 2222, doi:10.1029/2002JB001935.
Christoffersen, P., M. Bougamont, S. P. Carter, H. A. Fricker, and S. Tulaczyk (2014), Significant groundwater contribution to Antarctic ice streams hydrologic budget, *Geophys. Res. Lett.*, *41*, 2003–2010, doi:10.1002/2014GL059250.
Church, J. A., et al. (2013), Sea level change, in *Climate Change 2013: The Physical Science Basis. Contribution of Working Group I to the Fifth Assessment Report of the Intergovernmental Panel on Climate Change*, Cambridge Univ. Press, Cambridge, U. K., and New York.
Comiso, J. C. (2000), Variability and trends in Antarctic surface temperatures from in situ and satellite infrared measurements, *J. Clim.*, *13*(10), 1674–1696, doi:10.1175/1520-0442(2000)013<1674:vatias>2.0.co;2.
Conway, H., G. Catania, C. F. Raymond, A. M. Gades, T. A. Scambos, and H. Engelhardt (2002), Switch of flow direction in an Antarctic ice stream, *Nature*, *419*, 465–467.
Dukowicz, J. K., S. F. Price, and W. H. Lipscomb (2010), Consistent approximations and boundary conditions for ice-sheet dynamics from a principle of least action, *J. Glaciol.*, *56*(197), 480–496.
Engelhardt, H. (2004), Thermal regime and dynamics of the West Antarctic ice sheet, *Ann. Glaciol.*, *39*, 85–92.
Engelhardt, H., and B. Kamb (1997), Basal hydraulic system of a West Antarctic ice stream: Constraints from borehole observations, *J. Glaciol.*, *43*(144), 207–230.
Fried, M. J., C. L. Hulbe, and M. A. Fahnestock (2014), Grounding-line dynamics and margin lakes, *Ann. Glaciol.*, *55*(66), 87–96, doi:10.3189/2014AoG66A216.
Horgan, H. J., and S. Anandakrishnan (2006), Static grounding lines and dynamic ice streams: Evidence from the Siple Coast, West Antarctica, *Geophys. Res. Lett.*, *33*, L18502, doi:10.1029/2006GL027091.
Hulbe, C., and M. Fahnestock (2007), Century-scale discharge stagnation and reactivation of the Ross ice streams, West Antarctica, *J. Geophys. Res.*, *112*, F03S27, doi:10.1029/2006JF000603.
Jacobel, R. W., T. A. Scambos, C. F. Raymond, and A. M. Gades (1996), Changes in the configuration of ice stream flow from the West Antarctic Ice Sheet, *J. Geophys. Res.*, *101*(B3), 5499–5504, doi:10.1029/95JB03735.
Jacobel, R. W., T. A. Scambos, N. A. Nereson, and C. F. Raymond (2000), Changes in the margin of Ice Stream C, Antarctica, *J. Glaciol.*, *46*(152), 102–110.
Jacobel, R. W., B. C. Welch, D. Osterhouse, R. Pettersson, and J. A. MacGregor (2009), Spatial variation of radar-derived basal conditions on Kamb Ice Stream, West Antarctica, *Ann. Glaciol.*, *50*(51), 10–16.
Jacobson, H. P., and C. F. Raymond (1998), Thermal effects on the location of ice stream margins, *J. Geophys. Res.*, *103*(B6), 12,111–12,122, doi:10.1029/98JB00574.
Jenkins, A., P. Dutrieux, S. S. Jacobs, S. D. McPhail, J. R. Perrett, A. T. Webb, and D. White (2010), Observations beneath Pine Island Glacier in West Antarctica and implications for its retreat, *Nat. Geosci.*, *3*(7), 468–472, doi:10.1038/ngeo890.
Joughin, I., and R. B. Alley (2011), Stability of the West Antarctic ice sheet in a warming world, *Nat. Geosci.*, *4*(8), 506–513, doi:10.1038/ngeo1194.
Joughin, I., and S. Tulaczyk (2002), Positive mass balance of the Ross Ice Streams, West Antarctica, *Science*, *295*(5554), 476–480.
Joughin, I., L. Gray, R. Bindschadler, S. Price, D. Morse, C. Hulbe, K. Mattar, and C. Werner (1999), Tributaries of West Antarctic Ice streams revealed by RADARSAT interferometry, *Science*, *286*(5438), 283–286.
Joughin, I., S. Tulaczyk, D. R. MacAyeal, and H. Engelhardt (2004), Melting and freezing beneath the Ross ice streams, Antarctica, *J. Glaciol.*, *50*(168), 96–108.
Joughin, I., et al. (2005), Continued deceleration of Whillans Ice Stream, West Antarctica, *Geophys. Res. Lett.*, *32*, L22501, doi:10.1029/2005GL024319.
Kamb, B. (2001), Basal zone of the West Antarctic ice streams and its role in lubrication of their rapid motion, in *The West Antarctic Ice Sheet: Behavior and Environment*, *Antarct. Res. Ser.*, edited by R. B. Alley and R. A. Bindschadler, pp. 157–201, AGU, Washington, D. C.
Kyrke-Smith, T. M., R. F. Katz, and A. C. Fowler (2014), Subglacial hydrology and the formation of ice streams, *Proc. R. Soc. A*, *470*(2161), 20130494, doi:10.1098/rspa.2013.0494.
Le Brocq, A. M., A. J. Payne, M. J. Siegert, and R. B. Alley (2009), A subglacial water-flow model for West Antarctica, *J. Glaciol.*, *55*(193), 879–888.
Maule, C. F., M. E. Purucker, N. Olsen, and K. Mosegaard (2005), Heat flux anomalies in Antarctica revealed by satellite magnetic data, *Science*, *309*(5733), 464–467, doi:10.1126/science.1106888.

Paolo, F. S., H. A. Fricker, and L. Padman (2015), Volume loss from Antarctic ice shelves is accelerating, *Science*, *348*(6232), 327–331, doi:10.1126/science.aaa0940.
Pattyn, F. (2003), A new three-dimensional higher-order thermomechanical ice sheet model: Basic sensitivity, ice stream development, and ice flow across subglacial lakes, *J. Geophys. Res.*, *108*(B8), 2382, doi:10.1029/2002JB002329.
Price, S. F., R. A. Bindschadler, C. L. Hulbe, and I. R. Joughin (2001), Post-stagnation behavior in the upstream regions of Ice stream C, West Antarctica, *J. Glaciol.*, *47*(157), 283–294.
Price, S. F., R. A. Bindschadler, C. L. Hulbe, and D. D. Blankenship (2002), Force balance along an inland tributary and onset to Ice Stream D, West Antarctica, *J. Glaciol.*, *48*(160), 20–30.
Price, S. F., A. J. Payne, I. M. Howat, and B. E. Smith (2011), Committed sea-level rise for the next century from Greenland ice sheet dynamics during the past decade, *Proc. Natl. Acad. Sci. U.S.A.*, *108*(22), 8978–8983, doi:10.1073/pnas.1017313108.
Price, S. F., W. H. Lipscomb, M. J. Hoffman, M. Hagdorn, I. Rutt, A. Payne, and F. Hebeler (2015), CISM 2.0.0 Documentation. [Available at http://oceans11.lanl.gov/cism/data/cism_documentation_v.0.pdf.]
Pritchard, H. D., R. J. Arthern, D. G. Vaughan, and L. A. Edwards (2009), Extensive dynamic thinning on the margins of the Greenland and Antarctic ice sheets, *Nature*, *461*(7266), 971–975, doi:10.1038/nature08471.
Raymond, C. F. (2000), Energy balance of ice streams, *J. Glaciol.*, *46*(155), 665–674.
Raymond, C. F., K. A. Echelmeyer, I. M. Whillans, and C. S. M. Doake (2001), Ice stream shear margins, in *The West Antarctic Ice Sheet: Behavior and Environment*, edited by R. B. Alley and R. A. Bindschadler, pp. 137–156, AGU, Washington, D. C.
Retzlaff, R., and C. R. Bentley (1993), Timing of stagnation of Ice Stream-C, West Antarctica, from short-pulse radar studies of buried surface crevasses, *J. Glaciol.*, *39*(133), 553–561.
Robel, A. A., E. DeGiuli, C. Schoof, and E. Tziperman (2013), Dynamics of ice stream temporal variability: Modes, scales, and hysteresis, *J. Geophys. Res. Earth Surf.*, *118*, 925–936, doi:10.1002/jgrf.20072.
Scheuchl, B., J. Mouginot, and E. Rignot (2012), Ice velocity changes in the Ross and Ronne sectors observed using satellite radar data from 1997 and 2009, *Cryosphere*, *6*(5), 1019–1030, doi:10.5194/tc-6-1019-2012.
Schoof, C. (2004), On the mechanics of ice-stream shear margins, *J. Glaciol.*, *50*(169), 208–218.
Sergienko, O. V., and R. C. A. Hindmarsh (2013), Regular patterns in frictional resistance of ice-stream beds seen by surface data inversion, *Science*, *342*(6162), 1086–1089, doi:10.1126/science.1243903.
Shapiro, N. M., and M. H. Ritzwoller (2004), Inferring surface heat flux distributions guided by a global seismic model: Particular application to Antarctica, *Earth Planet. Sci. Lett.*, *223*(1-2), 213–224.
Shepherd, A., et al. (2012), A reconciled estimate of ice-sheet mass balance, *Science*, *338*(6111), 1183–1189, doi:10.1126/science.1228102.
Shreve, R. L. (1972), Movement of water in glaciers, *J. Glaciol.*, *11*, 205–214.
Siegfried, M. R., H. A. Fricker, M. Roberts, T. A. Scambos, and S. Tulaczyk (2014), A decade of West Antarctic subglacial lake interactions from combined ICESat and CryoSat-2 altimetry, *Geophys. Res. Lett.*, *41*, 891–898, doi:10.1002/2013GL058616.
Suckale, J., J. D. Platt, T. Perol, and J. R. Rice (2014), Deformation-induced melting in the margins of the West Antarctic ice streams, *J. Geophys. Res. Earth Surf.*, *119*, 1004–1025, doi:10.1002/2013JF003008.
Sutterley, T. C., I. Velicogna, E. Rignot, J. Mouginot, T. Flament, M. R. van den Broeke, J. M. van Wessem, and C. H. Reijmer (2014), Mass loss of the Amundsen Sea Embayment of West Antarctica from four independent techniques, *Geophys. Res. Lett.*, *41*, 8421–8428, doi:10.1002/2014GL061940.
Tulaczyk, S., W. B. Kamb, and H. F. Engelhardt (2000), Basal mechanics of Ice Stream B, West Antarctica 2. Undrained plastic bed model, *J. Geophys. Res.*, *105*(B1), 483–494, doi:10.1029/1999JB900328.
Tulaczyk, S., et al. (2014), WISSARD at subglacial Lake Whillans, West Antarctica: Scientific operations and initial observations, *Ann. Glaciol.*, *55*(65), 51–58, doi:10.3189/2014AoG65A009.
Van der Veen, C. J., K. C. Jezek, and L. Stearns (2007), Shear measurements across the northern margin of Whillans Ice Stream, *J. Glaciol.*, *53*(180), 17–29, doi:10.3189/172756507781833929.
van der Wel, N., P. Christoffersen, and M. Bougamont (2013), The influence of subglacial hydrology on the flow of Kamb Ice Stream, West Antarctica, *J. Geophys. Res. Earth Surf.*, *118*, 97–110, doi:10.1029/2012JF002570.
Vogel, S. W., S. Tulaczyk, B. Kamb, H. Engelhardt, F. D. Carsey, A. E. Behar, A. L. Lane, and I. Joughin (2005), Subglacial conditions during and after stoppage of an Antarctic Ice Stream: Is reactivation imminent?, *Geophys. Res. Lett.*, *32*, L14502, doi:10.1029/2005GL022563.
Whillans, I. M., and C. J. van der Veen (2001), Transmission of stress between an ice stream and interstream ridge, *J. Glaciol.*, *47*(158), 433–440.